

A mechanistic study of the physical quenching of Mg^* by C_2H_2 . Comparison of adiabatic and diabatic potential energy surfaces

A. Sevin, P. Chaquin and A. Papakondylis

Laboratoire de Chimie Organique Théorique¹, Université P. et M. Curie, Bâtiment F,
4 Place Jussieu, 75252, Paris Cedex 05, France

Received 25 July 1990

The mechanism of exciplex formation, along the low-energy potential energy surfaces (PESs) of the $Mg^*+C_2H_2$ system has been explored in the optimal C_{2v} geometry. Quasi-diabatic PESs were obtained from the MO-CI PESs, through calculation of the matrix elements of the $\partial/\partial R$ operator by a finite difference method. Although of qualitative grade these PESs clearly show the fundamental role of the charge-transfer PES which crosses, at short distance of interaction, the repulsive neutral (covalent) ones, asymptotically correlated with the excited metal + neutral acetylene.

1. Introduction

The understanding of the physical quenching of excited metal atoms (A^*) by small molecules M , i.e. electronic to vibrational, rotational and translational energy transfer, mainly depends on a couple of complementary limiting models [1]. The first one, originally proposed by Nikitin [2], and further improved by Bauer, Fischer and Gilmore [3], is based on the *diabatic* crossing, at short distance of interaction, of repulsive neutral (covalent) potential energy surfaces (PESs), A^*+M , with an attractive surface of ionic (charge-transfer, CT) character, A^++M^- . This model is well documented for systems in which the negative moiety M^- either is stable or, at least, not of too high energy with respect to that of the isolated neutral species to which they are asymptotically correlated. The second one, whose appellation "bond-stretch model" has been given by Hertel [4], is of concern when an *adiabatic* weak stabilization of a low-energy covalent state arises via a small relaxation of the neutral molecule, so as to increase the overlap of the valence MOs of the metal with its σ^* MOs. Examples of the first model are provided by the $Na+HF$ [5], $Li+N_2$ [6], $Mg+N_2$ [7] systems, while the second is illustrated by systems

such as Na [8] or $Mg+H_2$ [9] and Li or $Mg+CH_4$ [10]. In all the preceding cases, the physical quenching either competes, or is involved, with chemical quenching in which the electronic energy is transformed into chemical energy via bond breaking and/or making.

In this perspective, the system composed of excited Mg^* plus acetylene provides a vast field for both experimental and theoretical investigation. Previous studies have shown that in the parent system $Hg+C_2H_2$, the excited states $Hg(^3P_1)$ or $Hg(^3P_0)$ [11], essentially yield triplet acetylene, while when dealing with Li [12–14], Na , Al , Mg [15], acetylene to vinylidene rearrangements are observed, in which the metal participates. In the case of Li and Na , in the ground state (GS, lowest doublet PES), the reaction mechanism is essentially that of neutral acetylene, whereas when dealing with $Mg(^3P)$ and Al , the reaction is similar to that of the acetylene anion [15].

A theoretical SCF-CI study of the Mg +acetylene system reactivity, in the low energy $^1,^3P$ excited states of the metal, has been recently achieved [16]. It showed that the lowest energy singlet state of $Mg(^1P)$, yields a stable exciplex whose optimal geometry is an isosceles triangle (C_{2v}). The formation of this species is exothermic and the corresponding energy excess is large enough for inducing an hydrogen migration giving an intermediate vinylidene-mag-

¹ Part of the URA No. 506 of the CNRS.

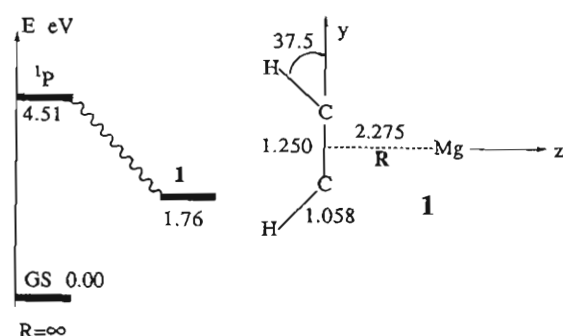


Fig. 1. Energy scheme for the formation of the 1^1B_2 exciplex **1**.

nesium, which, in turn, undergoes a C–Mg bond rupture, thus finally yielding vinylidene itself. The latter series of reactions competes with a possible insertion of Mg into a C–H bond. All this reaction pattern is ruled by a primary event: the formation of a deep potential energy well, of 2.75 eV calculated at the SCF+large Møller–Plesset CI level [17], whose energetics and geometry are displayed in fig. 1. The actual structure of the transient species **1** sets two linked questions: the geometrical parameters being typical of a charge-transfer moiety, i.e. $Mg^+ + C_2H_2^-$, rather than a neutral complex, i.e. $Mg^* + C_2H_2$, what is the actual mechanism of the electronic transfer? This problem puts to the fore the duality and possibly the complementarity of the models described in the forthcoming paragraphs. We will stay in this perspective, by affording in what follows a comparative analysis of the adiabatic and related diabatic PESs, calculated for the C_{2v} exciplex formation, our purpose being to propose a simple scheme showing the link between quantum mechanical calculations and classical ionic and covalent resonance forms.

2. Methodology

Ab initio SCF-CI calculations were achieved with the MONSTERGAUSS series of programs [18]. We used a basis set consisting of 6-31G functions [19]. A limited CI (including ≈ 100 functions) and direct diagonalization was then used for obtaining adiabatic surfaces. Then, in a second step, the coupling matrix elements $\langle \Psi_i | \partial/\partial R | \Psi_j \rangle$ were calculated between these states according to a general procedure

initially proposed by Lorquet et al. [20] (vide infra the appendix). These matrix elements can be exploited in two fashions. First, their magnitudes, as a function of the reaction coordinate R , indicate the actual region of diabatic crossings that occur when they are maximum^{#1}. Second, in the regions where avoided state crossings take place, the corresponding diabatic states can be obtained in the limiting approximation of a 2×2 problem, for which analytical solutions are available. In the latter case, the couple of adiabatic states Ψ_1 and Ψ_2 is transformed by an orthogonal transformation, via a $\theta(R)$ rotation, into the quasi-diabatic states χ_1 and χ_2 for which the diabatic condition: $\langle \chi_1 | \partial/\partial R | \chi_2 \rangle = 0$ is fulfilled. The rotation angle, $\theta(R)$, is obtained through numerical integration [19]:

$$\theta(R) = \int \langle \Psi_1 | \partial/\partial R | \Psi_2 \rangle dR.$$

The $\langle \Psi_1 | \partial/\partial R | \Psi_2 \rangle$ matrix elements have been calculated by a finite difference method. For each calculated point, the molecule geometry was frozen and the metal was placed at R and $R + \delta R$, with a δR microdisplacement (a value of 0.01 Å was generally used). Within this approximation, the problem is a one-dimensional one. Obviously, the corresponding results are only of qualitative grade, so that this study only pretends to provide an insight on the actual ionic to covalent interplay. More accurate calculations would afford more precise data about the actual energetics, but would not significantly change the main features of the overall electronic mechanism.

3. Adiabatic PESs

The adiabatic SCF-CI PESs, calculated for the low-energy singlet states of the system are displayed in figs. 2 and 3. A detailed analysis of the SCF-CI PESs relative to our system has already been made [16], so that in the coming sections we have restricted ourselves to only report the trends necessary for a comparison of adiabatic and diabatic PESs. With this aim, fig. 2 shows a selection of PESs obtained with C_2H_2 in its equilibrium geometry ($D_{\infty h}$ geometry, with $CC = 1.208$ Å and $CH = 1.058$ Å). The behavior

^{#1} A comprehensive discussion of the classical Landau–Zener model is found in ref. [21].

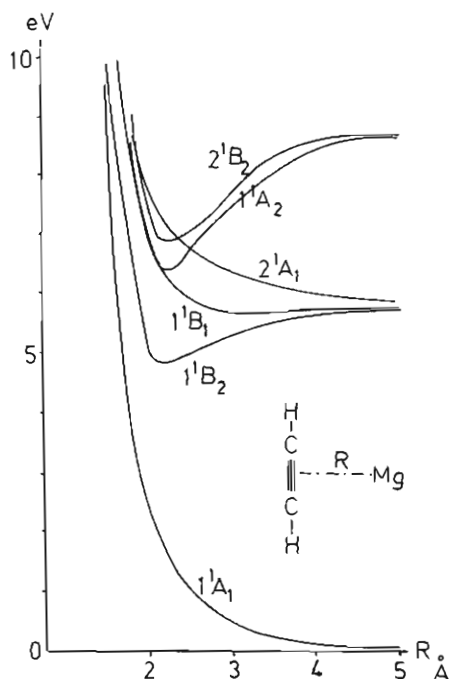


Fig. 2. Low-lying adiabatic PESs for the C_{2v} geometry, calculated with the equilibrium geometry of isolated C_2H_2 .

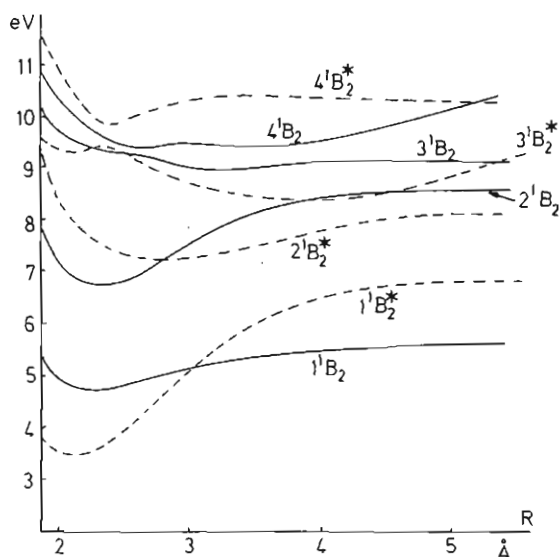


Fig. 3. Adiabatic PESs of B_2 symmetry. The starred PESs (dotted lines) refer to C_2H_2 with the optimized geometry I displayed in fig. 1.

of these states is essential in the coming discussion of exciplex formation.

At $R \approx 5 \text{ \AA}$, we first have the ground state (GS) of the system (asymptotic: $Mg(^1S) + C_2H_2(^1\Sigma_g^+)$), then we find the three components coming from Mg excited in its first 1P state, whose degeneracy is split at $R < 5 \text{ \AA}$ (asymptotic: $Mg(^1P) + C_2H_2(^1\Sigma_g^+)$). At higher energy, we only have reported the next state of B_2 symmetry (2^1B_2), and the first state of A_2 symmetry (1^1A_2). The latter state is asymptotically linked to a charge-transfer moiety, corresponding to $Mg^+(^2\Sigma^+) + C_2H_2^-(^2\Pi_g)$, with the unpaired electron located, at short R , in the π_x^* MO of C_2H_2 (in the reference frame defined in fig. 1). In the energetic range upon consideration, this state is the only one of this symmetry. For $2.5 < R < 5 \text{ \AA}$, it practically behaves as $1/R$ (in au), and becomes repulsive at short R , thus providing a good model for a "pure" CT species. At $R < 5 \text{ \AA}$, an important feature points out: the states of A_1 and B_1 symmetry are repulsive, while those of B_2 and A_2 symmetry yield very stable exciplexes. Of special interest is the quasi-parallel behavior of 1^1A_2 and 2^1B_2 in the range $2.5 < R < 5 \text{ \AA}$, which suggests the important role of a charged species of B_2 symmetry.

In fig. 3 are reported the calculated PESs for the first four states of B_2 symmetry. The full-line curves were calculated with C_2H_2 in its asymptotic equilibrium geometry (the same as in fig. 2), while the broken-line curves were obtained by setting C_2H_2 at the optimal geometry of the lowest energy exciplex I (fig. 1). The states corresponding to the latter case are labelled with an asterisk for the sake of clarity. Let us first examine the full-line PESs. At $R = 5 \text{ \AA}$, by order of increasing energy, one gets first the excited state of Mg, $1^1B_2(3s \rightarrow 3p_y)$, then 2^1B_2 whose CI eigenfunction consists in a mixture of a valence excited state of $C_2H_2(\pi_x \rightarrow \pi_x^*)$ (asymptotic: $Mg(^1S) + C_2H_2(^1\Sigma_u^+)$) and some Rydberg excitation of Mg ($3s \rightarrow 4p_y$) (asymptotic: $Mg(^1P) + C_2H_2(^1\Sigma_g^+)$). Very close in energy, we find a state, 3^1B_2 having the same CI leading components, but with inverted relative weights, thus indicating that in this region of the R coordinate, these states are undergoing an avoided crossing. The next state, 4^1B_2 , has a dominant CT character. Let us first examine the full-line curves. When R decreases, the upper states exhibit a strong mixing. As previously shown by the behav-

ior of 1^1A_2 , the CT state undergoes avoided crossings with 3^1B_2 and 2^1B_2 , as revealed upon examination of the CI eigenvectors, thus leading to the complex displayed adiabatic pattern. Very similar trends have already been found and discussed in the case of Li and Mg+N₂ [6,7]. In fact, the steep descent of the CT state induces the observed curvatures in the low-lying Rydberg and valence states, the phenomenon becoming important in the $2 < R < 4$ Å region.

When dealing with the PESs obtained with the exciplex geometry of C₂H₂ (structure 1), it is noteworthy that, at $R \approx \infty$, all PESs are located above those corresponding to the non-relaxed C₂H₂, the destabilization due to the geometrical changes acting as a constant energy increment. At $R \approx 5$ Å, the aforementioned crossing between the CT and the Rydberg states has already occurred, so that $3^1B_2^*$ has a dominant CT character. The last point is emphasized by the quasi-parallel behavior of 3^1B_2 and $4^1B_2^*$. It is worth focusing our attention on the PESs 1^1B_2 and $1^1B_2^*$. They cross each other at $R \approx 3$ Å, and we see that for $2 < R < 3$ Å, the deformation of C₂H₂ brings about an energy gain ≥ 1 eV, finally yielding the exciplex 1.

4. Diabatic PESs

The diabatic PESs of B₂ symmetry, obtained from the adiabatic ones of fig. 3, according to the general procedure described in the appendix, are displayed in fig. 4, with the same conventions and scale. We have restricted ourselves to the first two low-lying covalent states (neutral), and to the CT (ionic) states. The curves relative to the latter ones result from several diabatic crossings and have been fitted in order to behave continuously in the $3.5 < R < 5$ Å region. All these states are asymptotic, at $R \approx 5$ Å, to the adiabatic ones of the same geometry and characteristics.

Two distinct features point out: (i) The covalent states, for C₂H₂ in its two geometries, have a monotonous repulsive behavior. This trend has already been rationalized, and it is worth recalling these classical results. By considering the local system formed by the three p-type AOs (or hybrids), localized on

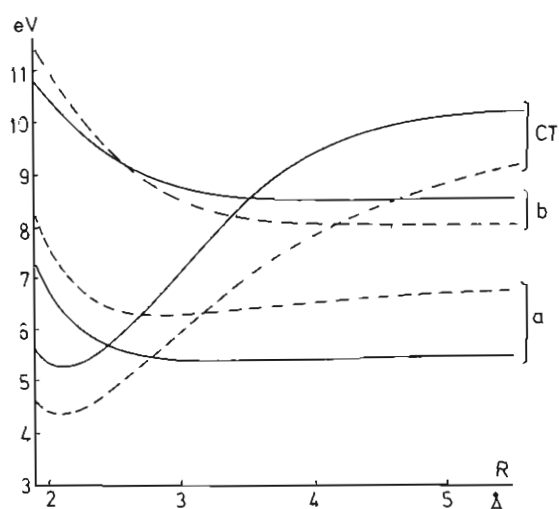


Fig. 4. Diabatic PESs of B₂ symmetry. (a) and (b) refer to the first and second valence state (neutral, or covalent), and CT to the charge-transfer state. See also the labels in fig. 2.

the carbon atoms (their combinations form π_z and π_z^*), on the one hand, and on Mg($3p_y$), on the other hand, one gets an isosceles three-electron-three-center system [22], for which it has been shown that the covalent interactions are repulsive [23,24], and lead to a "spin-forbidden" process [25], at all R distance. This effect which is partly ruled by the overlap between the three centers, is more pronounced for the Rydberg PESs (top covalent states), than for the valence PESs (bottom covalent states). Obviously, at short distance, the repulsion arising between the core electrons of each partner becomes noticeable and this effect superposes itself to the previous one. (ii) The ionic PESs exhibit a strong stabilization, both optimums being found at $R=2.1$ Å, the repulsive parts appearing at $R < 2$ Å. As when dealing with the adiabatic PESs, the relaxation of C₂H₂ provides the system with a stabilization of circa 1 eV, at $R=2.1$ Å. The diabatic crossings between covalent and ionic PESs occur at 2.5 Å for the non-relaxed geometry, and 3.2 Å for the relaxed one. When C₂H₂ has its resting geometry, the crossing point is located less than 0.5 eV above the asymptotic limit of the covalent PES, so that, taking into account the zero-point vibrational energy of the molecule, the system can easily reach this part of the reaction coordinate, and thus finally "jump" on the ionic surface, where fur-

ther rearrangement of C_2H_2 now occurs spontaneously.

With these findings, a simple mechanism for the formation of the exciplex can be proposed: starting from the lowest excited state of Mg, an easy approach drives the system to a region ($R \approx 2.5 \text{ \AA}$), where ionic character suddenly appears, without further activation energy, and then, the system spontaneously evolves through geometrical relaxation in good agreement with the classical Nikitin's model [2].

5. Conclusion

The examination of the diabatic PES clearly emphasizes the prominent role of the CT species, while in the adiabatic PESs, this phenomenon is partly masked by a progressive adaptation of the CI wavefunction through the various avoided crossings. Our procedure for obtaining the diabatic PESs, although rather crude and qualitative, nevertheless provides informations that are of simple chemical significance. Its routine use should greatly simplify the description of electronic processes, especially when stable exciplexes are formed, prior to any further evolution of the system.

Appendix

The following treatment is derived from the previous works of Lorquet et al. [19]. Let us calculate $\langle I | \partial/\partial R | J \rangle$ where $|I\rangle$ and $|J\rangle$ are CI eigenvectors of H_{el} . They are linear combinations of Slater determinants Ψ_i , built on the SCF MOs, Φ_r , themselves linear combinations of the basis AOs, χ_m .

$$|I\rangle = A_{1i}\Psi_1 + \dots + A_{ni}\Psi_n, \quad (1)$$

$$|J\rangle = A_{1j}\Psi_1 + \dots + A_{nj}\Psi_n, \quad (2)$$

with

$$|\Psi_i\rangle = |\Phi_1 \bar{\Phi}_1 \dots \Phi_r \dots\rangle \quad (k \text{ electrons}), \quad (3)$$

apart from normalization coefficients that have been skipped for the sake of simplicity, but that are to be taken into account in an actual calculation. There is a non-zero matrix element $\langle \Psi_i | \partial/\partial R | \Psi_j \rangle$ only if

$|\Psi_i\rangle$ and $|\Psi_j\rangle$ differ by one spin-orbital, say Φ_r , and Φ_s , respectively.

From (1) we get

$$\begin{aligned} \frac{\partial}{\partial R} |J\rangle &= \frac{\partial}{\partial R} A_{1j}\Psi_1 + \dots + \frac{\partial}{\partial R} A_{nj}\Psi_n \\ &+ A_{1j} \frac{\partial}{\partial R} \Psi_1 + \dots + A_{nj} \frac{\partial}{\partial R} \Psi_n. \end{aligned}$$

Multiplying by $\langle I |$ we obtain two kinds of terms (i) resulting from derivation of the CI coefficients $g_{(CI)}$; (ii) resulting from the derivation of the Ψ_i , $g_{(MO)}$. We will treat them separately.

(a) $g_{(CI)}$. Since the Ψ_i are eigenfunctions of H_{el} , one directly gets the non-zero terms:

$$g_{(CI)} = \sum_i^n A_{1i} \frac{\partial}{\partial R} A_{1j}. \quad (4)$$

We then use a finite displacement δR which yields

$$\frac{\partial}{\partial R} A_{1j} = \frac{1}{\delta R} (A'_{1j} - A_{1j}),$$

where the calculation is carried out at R (no prime) and $R + \delta R$ (prime), thus leading to

$$\begin{aligned} g_{(CI)} &= \frac{1}{\delta R} \sum_i^n A_{1i} (A'_{1j} - A_{1j}) \\ &= \frac{1}{\delta R} \left(\sum_i^n A_{1i} A'_{1j} - \sum_i^n A_{1i} A_{1j} \right). \end{aligned}$$

The second term in the large parentheses is nul, hence

$$g_{(CI)} = \frac{1}{\delta R} \sum_i^n A_{1i} A'_{1j}. \quad (5)$$

(b) $g_{(MO)}$. All symmetric terms such as $A_{1i} A_{1j} \langle \Psi_1 | \partial/\partial R | \Psi_1 \rangle$ are nul and the non-vanishing ones have the form $A_{ri} A_{sj} \langle \Psi_r | \partial/\partial R | \Psi_s \rangle$. Provided that Ψ_r and Ψ_s only differ by the spin-orbitals Φ_r and Φ_s , one has

$$g_{(MO)} = \sum_r \sum_{s \neq r} A_{ri} A_{sj} \langle \Phi_r | \frac{\partial}{\partial R} | \Phi_s \rangle. \quad (6)$$

The MOs Φ_r , Φ_s are written as

$$\Phi_r = B_{1r}\chi_1 + \dots + B_{mr}\chi_m, \quad \Phi_s = B_{1s}\chi_1 + \dots + B_{ms}\chi_m.$$

Upon derivation of Φ_s and then multiplication by Φ_r , we again obtain two kinds of terms, viz.

(a) those dealing with the coefficients of the

LCAO, which, after the finite displacement leading to eq. (5), yield in a similar way

$$g_{(\text{LCAO})} = \frac{1}{\delta R} \sum_k \sum_l B_{kr} B'_{ls} S_{kl}; \quad (7)$$

(b) those resulting from derivation of the AOs:

$$g_{(\text{AO})} = \sum_p \sum_{q \neq p} B_{pr} B_{qs} \langle \chi_p | \frac{\partial}{\partial R} | \chi_q \rangle. \quad (8)$$

To summarize all those contributions, we finally get

$$\begin{aligned} \langle I | \frac{\partial}{\partial R} | J \rangle &= \frac{1}{\delta R} \sum_r^n A_{ri} A'_{rj} & g_{(\text{CI})} \\ &+ \sum_r \sum_{r \neq s} A_{ri} A_{sj} \\ &\times \left(\frac{1}{\delta R} \sum_k \sum_l B_{kr} B'_{ls} S_{kl} \right) & g_{(\text{LCAO})} \\ &+ \sum_r \sum_{r \neq s} A_{ri} A_{sj} \\ &\times \sum_p \sum_{q \neq p} B_{pr} B_{qs} \langle \chi_p | \frac{\partial}{\partial R} | \chi_q \rangle & g_{(\text{AO})}, \end{aligned}$$

where the prime stands for $R + \delta R$ (a practical value of $\delta R \approx 0.01 \text{ \AA}$ was generally used). Two strategies exist depending on whether $g_{(\text{AO})}$ is explicitly calculated using the overlap matrix, or again obtained through finite difference. A Fortran program including both possibilities has been written; it is noteworthy that generally, the "all finite difference" methods yields more reliable results.

References

- [1] W.H. Breckenridge and H. Umemoto, *Advan. Chem. Phys.* 50 (1982) 325; W.H. Breckenridge, in: *Reactions of small transient species* (Academic Press, New York, 1983) p. 157.
- [2] E.E. Nikitin, *Theory of atomic and molecular processes in gases* (Oxford Univ. Press, Oxford, 1974); *J. Chem. Phys.* 43 (1965) 744; A. Bjerre and E.E. Nikitin, *Chem. Phys. Letters* 1 (1967) 179.
- [3] E. Bauer, E.R. Fischer and F.R. Gilmore, *J. Chem. Phys.* 51 (1969) 4173.
- [4] I.V. Hertel, *Advan. Chem. Phys.* 42 (1980) 325.
- [5] A. Sevin, P.C. Hiberty and J.M. Lefour, *J. Am. Chem. Soc.* 109 (1987) 1845.
- [6] A. Sevin, P. Chaquin, L. Hamon and P.C. Hiberty, *J. Am. Chem. Soc.* 110 (1988) 5681.
- [7] P. Chaquin and A. Sevin, *Chem. Phys.* 123 (1988) 351.
- [8] A. Sevin and P. Chaquin, *Chem. Phys.* 93 (1985) 49.
- [9] P. Chaquin, A. Sevin and H.T. Yu, *J. Phys. Chem.* 89 (1985) 2813; B.H. Lengsfeld, P. Sax and D.R. Yarkony, *J. Chem. Phys.* 81 (1984) 4549.
- [10] P. Chaquin, A. Papakondylis, C. Giesner-Prettre and A. Sevin, *J. Phys. Chem.*, in press.
- [11] H.R. Wendt, H. Hippler and H.E. Hunziker, *J. Chem. Phys.* 70 (1979) 4044.
- [12] C. Pouchan, *Chem. Phys.* 111 (1987) 87.
- [13] V. Bonačić-Koutecký, private communication.
- [14] M.T. Nguyen, *J. Phys. Chem.* 92 (1988) 1426.
- [15] S. Sakai and K. Morokuma, *J. Phys. Chem.* 91 (1987) 3661.
- [16] P. Chaquin, A. Sevin and A. Papakondylis, *Chem. Phys.* 143 (1990) 39.
- [17] B. Huron, J.P. Malrieu and P. Rancurel, *J. Chem. Phys.* 58 (1973) 5745; J.P. Malrieu, *Theoret. Chim. Acta* 62 (1982) 163; S. Evangelisti, J.P. Daudey and J.P. Malrieu, *Chem. Phys.* 75 (1983) 91.
- [18] M. Peterson and R. Poirier, MONSTERGAUSS, Department of Chemistry, University of Toronto, Toronto, Canada (1981).
- [19] M.M. Francl, W. Pietro, W.J. Hehre, J.S. Binkley, M.S. Gordon, D.J. DeFrees and J.A. Pople, *J. Chem. Phys.* 77 (1982) 3654; M.S. Gordon, J.S. Binkley, J.A. Pople and W.J. Pietro, *J. Am. Chem. Soc.* 104 (1982) 5039; W.J. Pietro, M.M. Francl, W.J. Hehre, D.J. DeFrees, J.A. Pople and J.S. Binkley, *J. Am. Chem. Soc.* 104 (1982) 5039.
- [20] C. Galloy and J.C. Lorquet, *J. Chem. Phys.* 67 (1977) 4672; M. Desouter-Lecomte, D. Dehareng and J.C. Lorquet, *J. Chem. Phys.* 86 (1987) 1429, and references therein.
- [21] J.B. Delos and W.R. Thorson, *Phys. Rev. A* 6 (1972) 728.
- [22] F.A. Matsen, *J. Phys. Chem.* 68 (1964) 3282.
- [23] K. Yamaguchi, *Chem. Phys. Letters* 28 (1974) 93; K. Yamaguchi and T. Fueno, *Chem. Phys. Letters* 38 (1976) 52.
- [24] S. Nagase, K. Takatsuka and T. Fueno, *J. Am. Chem. Soc.* 98 (1976) 3838.
- [25] V. Bonačić-Koutecký, J. Koutecký and L. Salem, *J. Am. Chem. Soc.* 99 (1977) 842.